# Supplementary Information for paper *"Urban hydrogeology: transport routes and mixing of water and solutes in a groundwater influenced urban lowland catchment"*

**Contents**



## 1. Information over the rain water collection system, the groundwater drainage system and the sewage system in the study area

Polder Geuzenveld has a separated system of sewer and rain drainage system. Groundwater drainage system is also planted to drain excessive groundwater into surface water. Figure SI 1.1 and Figure SI 1.2 show the groundwater (purple line) drainage and rain water drainage (blue lines) systems. The red line is the main sewer system that transport municipal water to the treatment plant.

The precipitation on the roofs is collected by the pipes installed on the buildings, and transported to the rain water manhole, that is connected to the ditches. Precipitation on the street is considered as runoff that flows into the drainage system which also ends up in the manhole then flow into the ditches.

The outlets are the places where the pipes end. At the locations of the outlets, water qualities are influenced depends on it is rain water drainage outlet or groundwater drainage outlet. There are rain water outlets in the west and middle ditches, especially location W1 and M1 (where A and G for survey sampling, rain water influenced water sample were collected). The groundwater drainage system only placed in the middle of the polder with the outlets open in the north (1 outlet) and south ditches (3 outlets). The two outlets in the west and middle ditch are hidden. There are no outlets open in the East ditch, which leave location E1 and E2 out of influences from runoff and drain water.

The manholes accordingly belong to rain water, groundwater drainage and sewer water. Each of them has their elevations refer to N.A.P and codes recorded in Waternet's water system. The outlook of the manholes is shown in Figure SI 1.3.

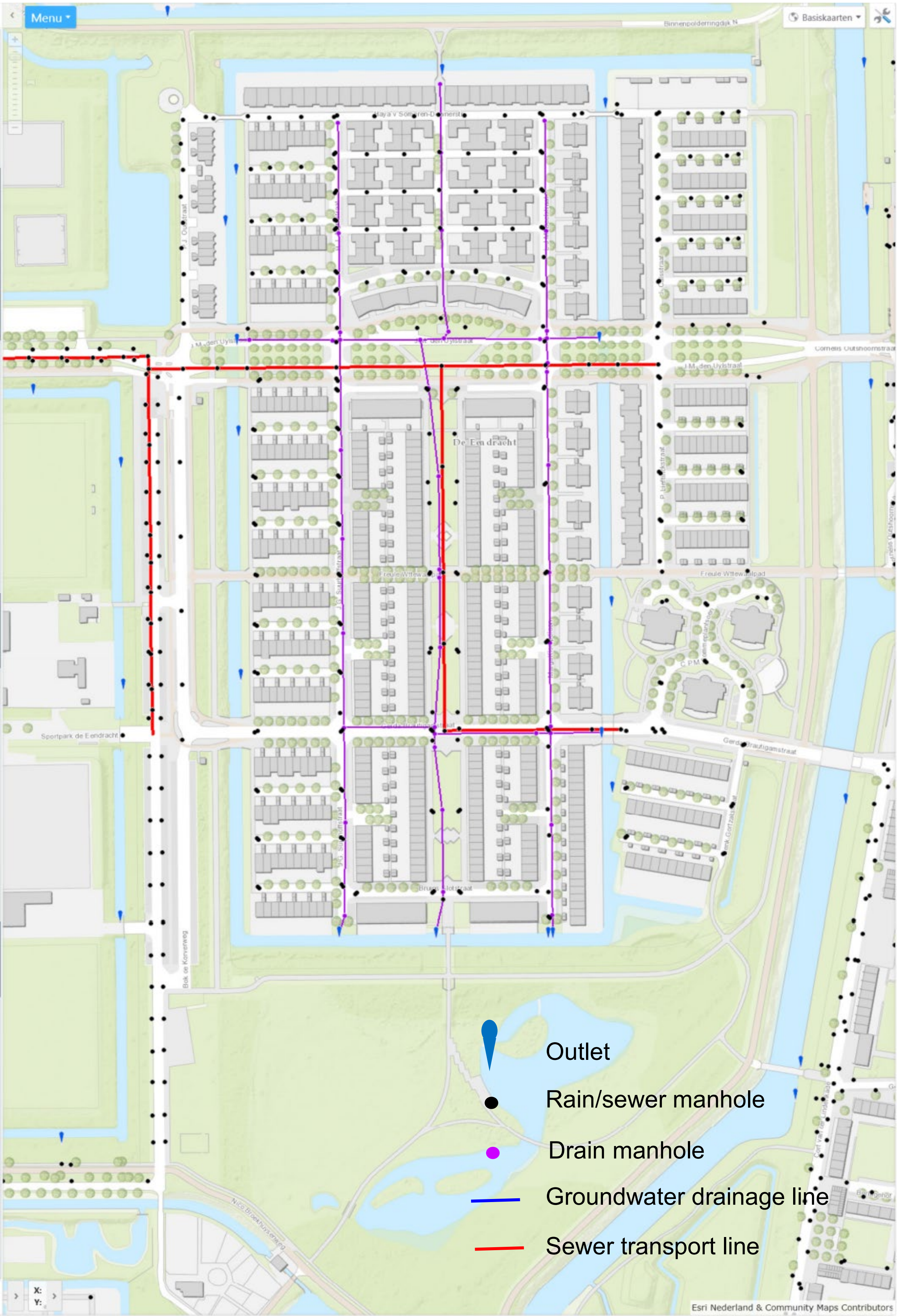


Figure SI 1.1 Groundwater drainage system and the sewer system

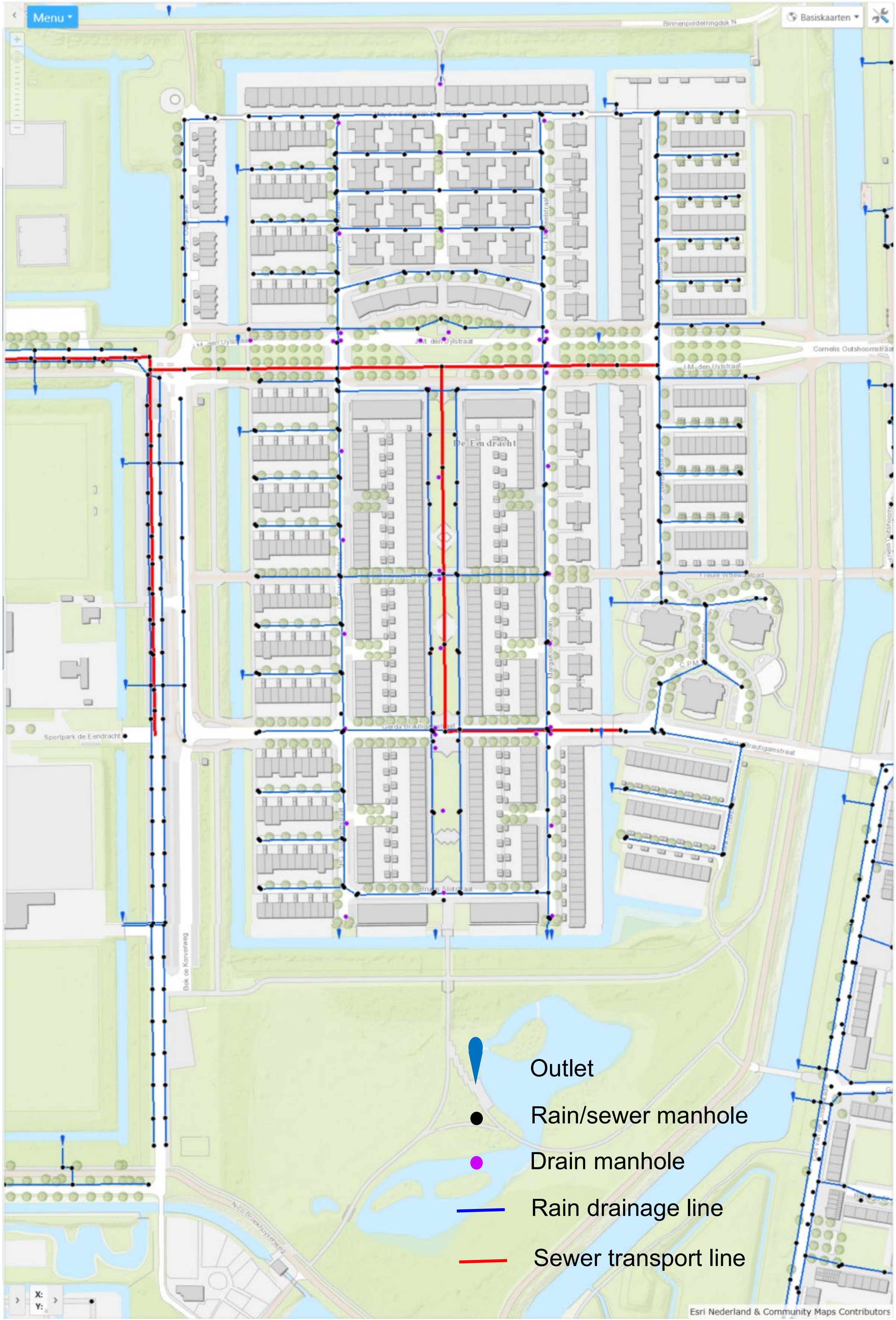


Figure SI 1.2 Rain water drainage system and the sewer system

Figure SI 1.3 Example of a manhole of the groundwater drainage system (the dead fish indicates the possible back flow from the ditch to the drain manhole)

## 2. Data collection and data treatment

### Groundwater sampling

Groundwater in the polder (GWS, shallow piezometers) and around the polder (GWD1 and GWD2, deeper groundwater at ~1 km distance) was sampled twice during the monitoring campaign. Once in the dry season (May 2017) and once in the wet season (November 2017). Groundwater wells were purged removing at least three times of the stagnant water volume in the tubes using peristaltic pumps. The pump was connected to a flow through cell, and the pH, $O_2$, and EC were measured on-site until stabilization. Additionally, alkalinity as $HCO_3$ was measured on-site using an AL-DT HACH digital titration set. Parameters measured included pH, $O_2$, EC, $HCO_3$, Cl, $^{222}Rn$, and $\delta^{13}C$-DIC.

### Sampling the flow routes during a spatial survey

Five sample bottles were filled at each sampling point. Three samples were filtered through 0.45 µm filter for analysis at the joint TNO/University Utrecht Central Environmental Laboratory (Utrecht Castel). The samples that were pre-acidified with sulfuric acid were used for the analysis of ortho-$PO_4$, $NH_4$ (NEN-EN-ISO-11732 and NEN-EN-ISO-15681-2, respectively), and for Dissolved Organic Carbon(DOC) (NDIR). The samples that were pre-acidified with nitric acid was analyzed by ICP-MS for metals and TP. The non-acidified sample was used to measure $NO_3$, Cl, and $SO_4$, using IC. The additional two samples were treated as regularly done by the Waternet water board who do not typically filter the samples. TP was analyzed photometrically (NEN-EN-ISO 15681-2, 2005) and $NH_4$ using a discrete analyzer (NEN ISO 15923-1). Analysing TP and $NH_4$ in both labs was intended for quality control and for matching the long-term grab sampling time series from Waternet with the results of this spatial survey. In addition, comparing TP concentrations (filtrated and non-filtrated) and ortho-P concentrations helped to identify species of phosphorus among locations. 72% of the samples had an ion balance error of < 5%. Large deviations were only found for the samples that contained low-mineralized runoff water, where measurement errors easily lead to deviations > 5%.

### Short and long term water quality monitoring

During the monitoring campaigns, each sample was collected under random hydrological conditions following a systematic sampling design with fixed sampling moments in time. The weekly and biweekly samples at the 8 new locations yielded values of EC, $O_2$, pH, $HCO_3$, and Cl that were measured on-site. The database contains results of EC, pH, and $O_2$, suspended solids (SS), Ca, Cl, $HCO_3$, $SO_4$, $NH_4$, and TP. The collected samples were preserved onsite according to the standard NEN-EN-ISO 56667-3 (2012). Cl, $NH_4$, $SO_4$, and Ca were filtered at site. TP and Ca were acidified with respectively sulfuric acid and nitric acid. The field parameters EC, pH, and $O_2$ were measured with a Hanna HI9828 multi parameter probe and analyzed according to the standards NEN-ISO 7888 (EC), NEN-EN-ISO 10523 (pH) and in-house method ($O_2$). The following parameters were analyzed at the laboratory: SS is a filtration method and analyzed according to standard NEN-EN 872; $HCO_3$ is a titration method and measured with a Metrohm titrator, according to an in house method; Cl, $NH_4$, and $SO_4$ were measured with a discrete Analyzer (DA) according to the standard NEN-ISO 15923-1; TP was measured with a continuous flow auto analyzer (AA) according to the standards NEN-EN-SIO 15681-2 and NEN 6645; Ca was measured with an ICP-MS according to the standard NEN-EN-ISO 17294-2. For quality assurance, we checked the ion charge balance of this dataset using following Appelo, et al. (2010)[1]

**$\delta^{13}$C-DIC and $^{222}$Rn sampling**

$\delta^{13}$C-DIC samples of the surface water at locations M2, E2, and B' were prepared in 100 mL brown glass bottles and stabilized with mercury chloride in the field. $\delta^{13}$C-DIC samples for groundwater were taken from May 28th-30th 2016 with a similar sampling procedure. $\delta^{13}$C in dissolved inorganic carbon was measured using mass spectrometry (Thermo Finnigan Isotope Ratio Mass Spectrometers). $\delta^{13}$C-DIC is reported as $\delta^{13}$ (in ‰) using the universal δ notation with VPDB (Vienna Pee Dee Belemnite) as standard for marine carbonates. We applied the RAD-H2O (Durridge Company, 3D printed aerator cap) to analyze $^{222}$Rn concentrations in water. $^{222}$Rn samples were taken without filtration in 250 mL glass vials and were analyzed in the field. Before the measurement, the RAD-H2O system had to be purged to remove potential $^{222}$Rn residuals and to get the humidity of air lower than 10%. Then the glass vial was connected to the cap that formed a loop connection with the RAD 7 detector. Desiccant dehumidifier was used to keep the loop dry. Following the protocol, it first aerated the system for 5 minutes to achieve an equilibrium of 222Rn in the water and air in the whole system. Subsequently, 4 measuring cycles of 5 minutes each were done. After this, we used the RAD 7 data processing software (Capture) to get an average $^{222}$Rn concentration value corrected for humidity.

## 3. Calculating the Antecedent Precipitation-Evaporation Index

For analyzing the surface water composition during different hydrological conditions, we divided the samples based on the APEI at the moment of sampling. We collected precipitation and potential evaporation (Makkink, 1957)[2] data from the Schiphol Airport KNMI (The Royal Netherlands Meteorological Institute) weather station, which is located 9 km south from polder Geuzenveld. We divided the hydrological condition of the catchment for each day into 4 classes from driest (class 1) to wettest (class 4) based on the calculated APEI values as below, following the procedure of Rozemeijer et al., 2010[3]:

$$APEI_t = APEI_{t-1} \times Decay\ rate + (Precipitation - Evaporation)_t \quad (1)$$

APEIt is APEI (mm) at day t. Precipitation and evaporation are both daily records in mm (KNMI, http://www.knmi.nl). We chose a decay rate of 0.76 in this study area, based on the best fit between daily and weekly accumulated APEI values with known pumping volumes at the principal outlet of our polder system, and the recession line of the water levels.

We strived for a reasonable division of the periods with dry, intermediate, and wet conditions and used expert judgement to derive the following distribution of time over the 4 wetness classes: 12%, 13%, 50%, and 25% covering the period 2006-2017 (Fig. SI 3.1). The

[1] Appelo, C.A.J. and D. Postma. Geochemistry, groundwater and pollution (2nd edition). CRC Press, UK, 2010.

[2] Makkink, G.F.: Testing the Penman formula by means of lysimeters. Journal of the Institution of Water Engineers and Scientists, 11, 277-288, 1957.

[3] Rozemeijer, J.C., van der Velde Y., van Geer F., de Rooij G. H., Torfs P.J.J.F., Broers H.P.: Improving Load Estimates for $NO_3$ and P in Surface Waters by Characterizing the Concentration Response to Rainfall Events. Environmental Science & Technology, 44 (16): 6305–6312, 2010.

associated APEI values of each class were: APEI <= -10 for class 1, -10 < APEI <= -5 for class 2, -5 < APEI <= 9 for class 3, and APEI > 9 for class 4. The distribution of the wetness classes gives a good fit between pumping rates and weekly APEI (Fig. SI 3.2) and yields an acceptable and credible distribution of the wetness classes over the seasons and in relation to periods with large precipitation events. The wettest period with accordingly higher classes are more found in autumn and winter and the driest are in spring and summer.

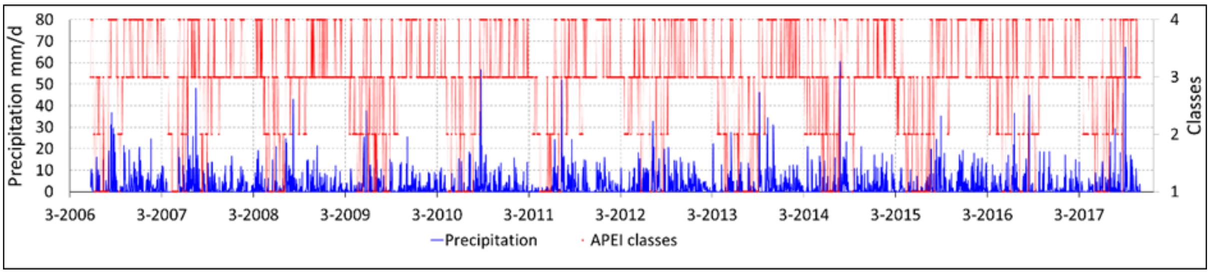


Figure SI 3.1 APEI wetness classes with precipitation from 2006 to 2017, left y-axis is precipitation in mm/d (blue color), right y-axis is APEI classes (red color).

We tested the APEI indicator against the weekly pumping rate for the 2006-2017 period. A small number of values of Q (weekly discharge rate) > 30000 $m^3$/week were considered improbable given the total capacity of the pumps in the pumping house, and the known pumping schedule of the water board, were distracted from the analysis. The graph indicates that pumping is much less in dry periods with negative weekly APEI than in wet periods with positive weekly APEI.

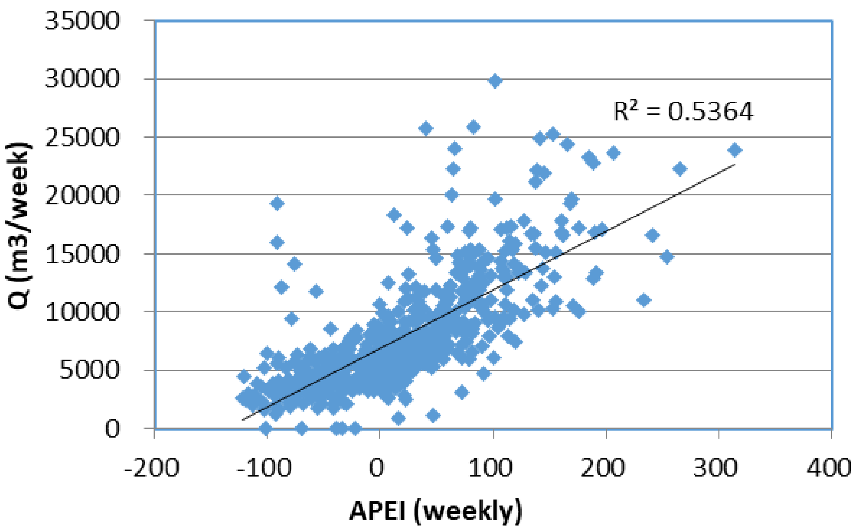


Figure SI 3.2 weekly cumulative pumping rates with weekly cumulative APEI of polder Geuzenveld

## 4. Boxplots of the 2017 survey and the results of the principle component analysis

Table SI 4.1 Cumulative explained variance of the principle components

| | PC1 | PC2 | PC3 | PC4 |
|---|---|---|---|---|
| Scaled (original value-mean)/SD | 0.57 | 0.72 | 0.79 | 0.85 |
| Scaled & normalized (box-cox in R program) | 0.66 | 0.76 | 0.83 | 0.89 |

The correlation of the variables to each component is not shown, as they are almost all correlated to the first component.

## Group 1:

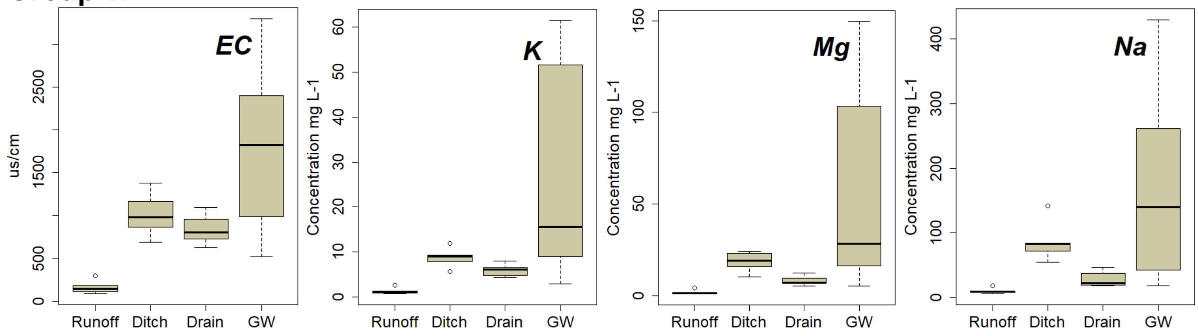


## Group 2:

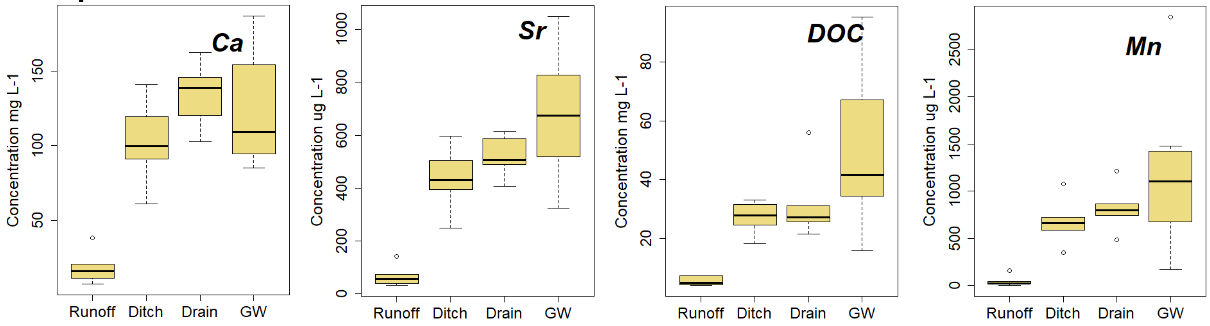


## Group 3:

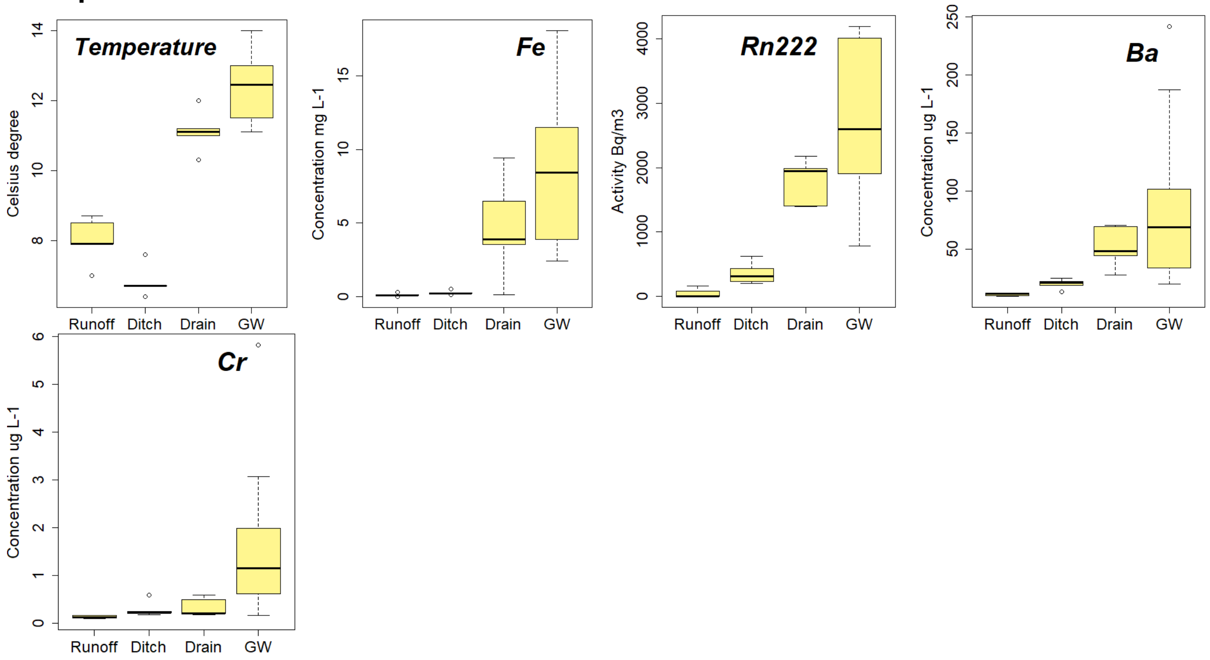


## Group 4:

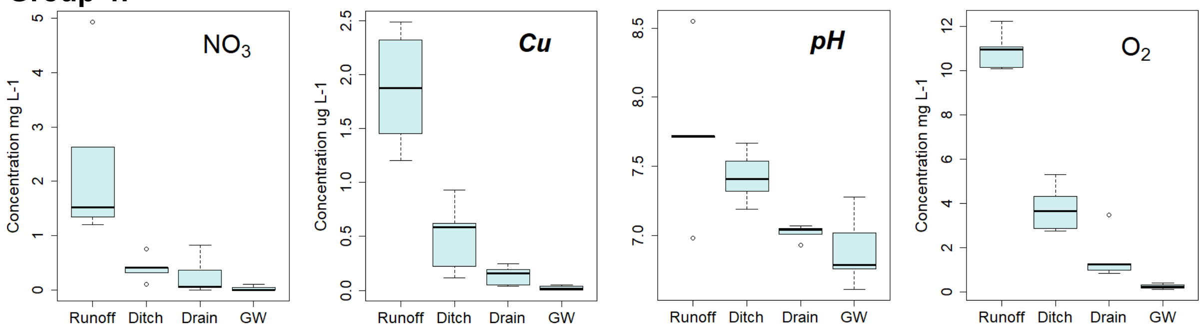

**Group 5:**

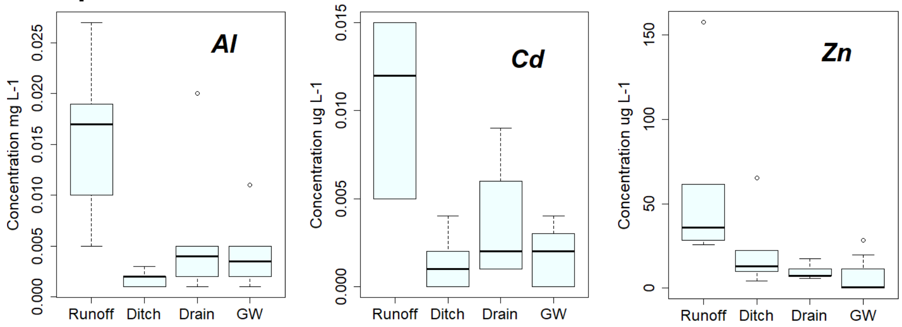


**Group 6:**

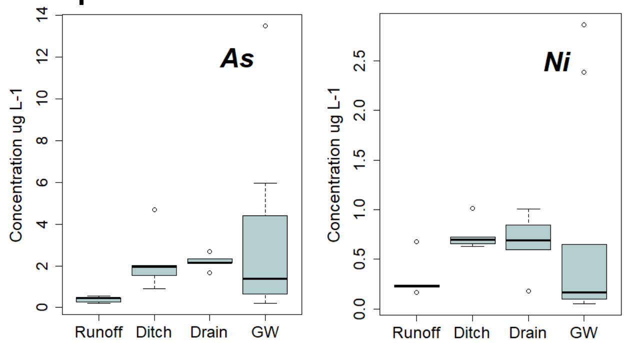


Figure SI 4.1 Concentrations of the water quality variables collected during the 2017 survey, ordered using the groups from the PCA resullts below as a function of the flow routes sampled: runoff (observation number n = 5), ditch water (n = 5), drain water (n = 5), and groundwater (n = 10).

## 5. Mixing processes using a Piper diagram

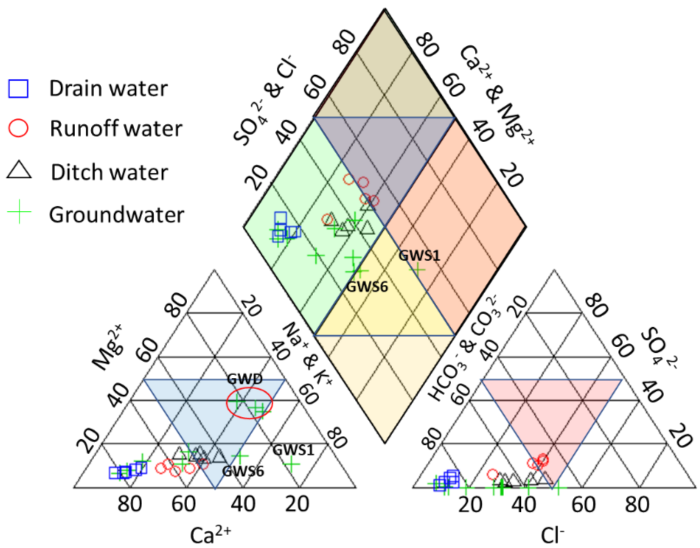


Figure SI 5.1 Piper diagram of major ions in drain, runoff, ditch water and groundwater

We primarily used a PCA approach to unravel the mixing processes in our urban catchment, but add a Piper diagram here which confirms the main mixing processes that we identified in the main text. Ditch water is centered in the diagram and is a mixture between the 3 main flow routes: seepage of groundwater, and inflow of drain and rain water. The Piper diagram also confirms our finding the shallow groundwater at locations GWS 1 and GWS 6 in the southwest polder show some similarity with the deeper groundwater and reveals a slightly brackish signature in this shallow water with higher Na and Cl. In the main text, we argue this to be the result of seepage through the connection between the deep and shallow groundwater in the southwest part of the polder where the tidal channel is located. The other shallow wells show large similarity to the drain water, and mainly fresh infiltrated water is transported by this shallow system of groundwater and drains.

## 6. Pictures of the setting of the locations where water from the canals was sampled during the 2016-2017 water quality surveys

| Location W1 | Location W2 |
|---|---|
|  |  |
| **Location M1** | **Location M2** |
|  |  |
| **Location E1** | **Location E2** |
|  |  |

| Location B’ | Location B |
|---|---|
|  |  |
| **Location Pump** | **The park** |
|  |  |

## 7. Iron-hydroxides precipitation

The following pictures show the iron-hydroxides precipitation phenomenon, during dry and wet period. Iron-hydroxides are indicated by the brown color in the water bodies. In the dry period, the water bodies had brownish color and low transparence. In the wet period (which just after ample rain), the appearance of the water was still brownish while only the upper part is more transparent made the iron precipitant in the deeper water or on the bottom visible. Iron precipitants also clearly visible in the aeration sampling plate in the water, which bubbles water to repel dirt, that brought $O_2$ into water and caused dissolved iron precipitated on the plate.

Figure SI 7.1 Iron precipitation on an aeration sampling plate

## 8. Information about the precipitation pattern during out November 2017 spatial water quality survey

Ample rainfall happened before and during the survey (2017-11-28 to 2017-12-01) of ditch, drain, rain and groundwater. Ditch, drain and rain water were sampled between 11-28 and 11-29, and groundwater were mostly sampled on 11-30 and 12-01. The ample rainfall events may cause the shallow groundwater influenced by rain water infiltration.

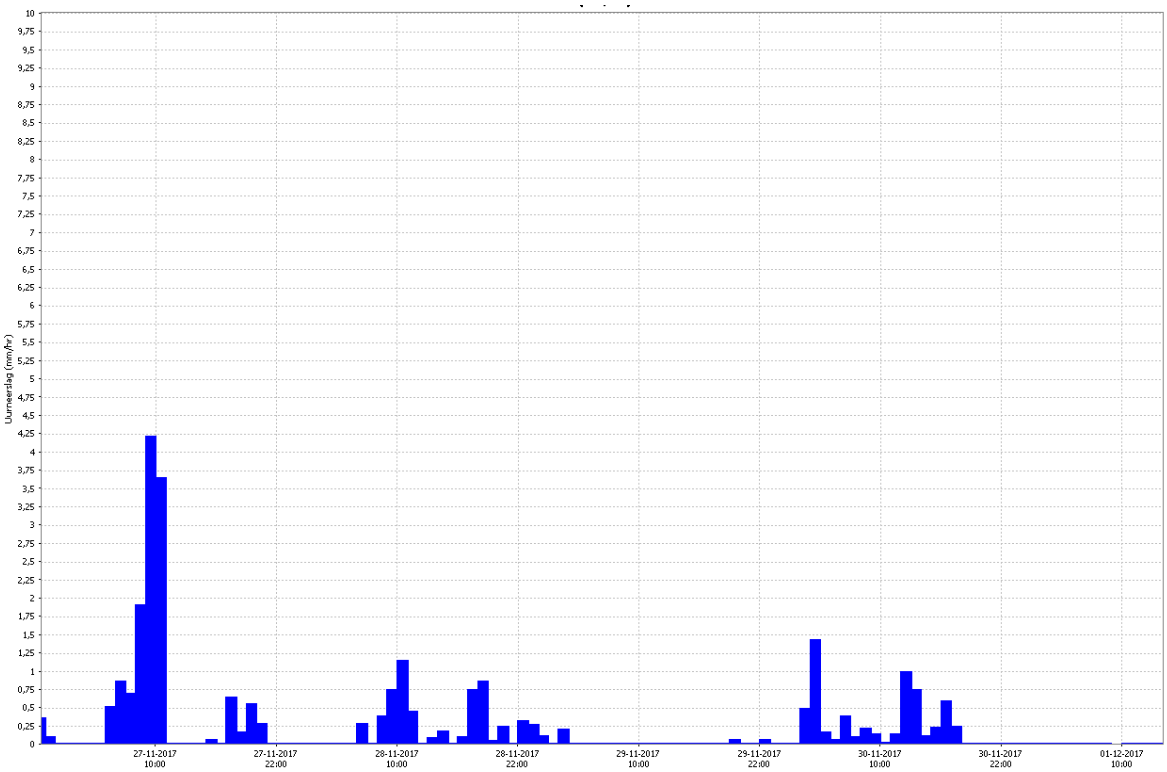


Figure SI 8.1 Precipitation around the survey sampling